INTERNATIONAL JOURNAL OF
AUTOMOTIVE SCIENCE AND TECHNOLOGY

2022, VOL. 6, NO: 3, 265-274 www.ijastech.org e-ISSN: 2587-0963

An Examination of the Vibrational Characteristics of a Diesel Engine Connecting Rod Using Modal Analysis

Bahri Şamil Korkmaz[1], Abdurrahman Karabulut[1*]

0000-0002-2798-6741, 0000-0002-7663-2579

[1] *Mechanical Engineering Department, Faculty of Technology, Afyon Kocatepe University, Afyonkarahisar, 03200, Turkey*

Abstract

In this study, a connecting rod that belongs to a diesel test engine is examined with an experimental method and the Finite Element Method (FEM). The purpose of the experimental method is to obtain the Frequency Response Function. The graph of this function provides the necessary vibrational qualifications of the connecting rod. Obtained vibrational characteristics can be considered as natural frequencies, damping ratios and mode shapes that belong to these vibrational modes. While natural frequencies can be obtained with both of these methods, mode shapes could only be produced with FEM. The natural frequencies that are obtained with experimental method is determined for the first mode as 1,25 Hz, for the second mode as 4,38 Hz, and for the third mode as 8,13 Hz. The natural frequencies that are obtained with FEM is determined for the first mode as 0,04575 Hz, for the second mode as 8,3861 Hz, and for the third mode as 8,9434 Hz. Considering the frequency range of the connecting rod, this study shows that the natural frequency values which is determined from this study and any frequency value of the connecting rod while the engine is running would not coincide. Besides damping ratios are calculated for the first mode as 19,766 %, for the second mode as 8,0116 %, and for the third mode as 3,4839 %. It is determined which modes have bending and torsion mode shapes. The results provide the useful information about the weaknesses and the vibrational qualifications that has to be improved in terms of dynamical and structural analysis of the connecting rod or engine itself.

Keywords: Modal analysis, Connecting rod, Frequency response function.

Research Article

https://doi.org/10.30939/ijastech..1053850

Received 05.01.2022
Revised 25.04.2022
Accepted 20.05.2022

* Corresponding author
Abdurrahman Karabulut
akarabulut@aku.edu.tr
Address: Mechanical Engineering Department, Faculty of Technology, Afyon Kocatepe University, Afyonkarahisar, Turkey
Tel: +90272 218 2532

1. Introduction

Internal Combustion Engines (ICE) convert the chemical energy that different types of fuels have into mechanical energy usually via the rotation of a shaft. [1] While there have been developments in the details of the ICE for over 130 years, the main structure and operating logic of ICE have not significantly changed. For instance, nearly all the engines that are still in use today are four-stroke. [2] As it is known, the fact that the engine is four-stroke is related to the reciprocating motion of the pistons. Commonly, ICEs are produced with pistons designed as reciprocating or lately developed rotary types. In these definitions, the key factor is the movement of the piston. [3] The connecting rod is a machine part that transfers the motion of the piston to the crankshaft. Tensile, compressive, and bending stresses may occur during connecting rod movement. In theory, the connecting rod consists of three parts: Big end, small end, and shank. In many cases shank may be exposed to tensile and compressive stress.

A mechanical system or structure has dynamic characteristics such as natural frequencies, mode shapes, and damping ratios. The process of determining these characteristics is called Modal Analysis. Experimental Modal Analysis is performed with particular equipment. With this equipment, a time response is obtained. The time response is a graph that shows the deformation data of the system or structure depending on time. Frequency Response Function (FRF) converts the same graph to the frequency domain by using time signals. Experimental Modal Analysis provides an FRF graph. In this graph, the points that correspond to the peaking points show the natural frequency values. While it is very hard to determine how many modes the system experimented has, FRF reveals the number of modes almost precisely. [4]

More and Mishra aimed to define the vibrational characteristics of the connecting rods that have been produced from two separate materials. Experimental Modal Analysis is carried out with an impact hammer and accelerometers to the connecting rods that are produced from 16MnCr5 carbon steel ve Aluminium LM9 materials. The results of this experiment are compared with the Finite Element Method solutions. [5]

Nale and Kulloli carried out the Modal Analysis via an FFT Analyser and FEM. They aimed to design a more convenient connecting rod in terms of weight and economy. Also, a program called Optistruct which can examine numerous amount of design parameters at once has been used. Obtained Modal Analysis results evaluated in Optistruct. According to this evaluation, the connecting rod has been redesigned with desired vibrational characteristics. [6]

Tong et al. examined a connecting rod that has been produced from ZG35CrMo material. That connecting rod belongs to a mud pump. In Experimental Modal Analysis mostly the experimental setup is prepared according to the theory that recommends the experimented machine parts should have 6 degrees of freedom so that the machine part rotates and translates in all possible directions. Contrary to that, the connecting rod is connected with the crankpin and crosshead pin, which produces a system that is examined in the operating conditions. The examined system is not only the connecting rod but all the system that connecting rod has been connected. The results show that the stress distribution is generally explicit in the center of the connecting rod as much as in the connected areas of the connecting rod. That leads to the fact that conventional design concepts should not be deviated from. [7]

Manda et al. carried out the modal analysis in similar conditions to the study of Tong et al. with the ANSYS program. They specify 6 points upon the connecting rod and determine the magnitudes of deformations and which frequency values cause these deformations. They also created and showed the graphical representations related to the frequency and deformation values. [8]

Kumar has studied the structural properties of the piston and piston ring. He proposed a SiC reinforced ZrB2 composite material and compared it with an aluminum alloy piston. Not only the stress analysis but also the Modal analysis has been performed. He examined these two materials in terms of pressure and temperature. [9]

Zheng et al. have performed a Modal Analysis on the piston of the WP10.290 diesel engine. They carried out this study to find natural frequencies and mode shapes with the ANSYS program. [10]

Patil et al. have performed Modal Analysis on a camshaft. Camshafts can easily be exposed to varying loads and vibrations. Natural frequencies have been founded with the analytical method called Dunkerley's Method and also with FEM. Besides, they performed fatigue analysis to avoid fatigue failures. [11]

Thriveni and Chandraiah have also performed a Modal Analysis of a different camshaft. Catia program is used to perform Modal Analysis. [12]

Naghate and Patil have designed an engine mounting bracket to select two different materials. They performed a Modal Analysis on the engine mounting bracket with FEM. Aluminum and magnesium alloy engine mounting brackets are compared in terms of natural frequencies, and mode shapes. Also Von-Mises stress and Total deformation values have been founded. They aimed to reduce the weight of the bracket. [13]

Nuraini et. al. have studied the Modal Analysis of a piston engine with finite element and boundary element methods. They obtained vibration data and use it for noise analysis. Therefore engine noises are examined with the contribution of the results of Modal Analysis. [14]

Chaudhary et. al. examined an engine cylinder block. Modal Analysis has been performed in order to place a knock sensor optimally on the cylinder block. Natural frequencies, damping specifications, and mode shapes have been found. Therefore optimum position on the cylinder block to place the knock sensor has been spotted. [15]

In this study vibrational characteristics of a connecting rod that belongs to a diesel engine are examined with experimental modal analysis and ANSYS Modal module. The results that are obtained in either way are evaluated according to the different scenarios for the different results. Besides, it is aimed that examining the effects of revolution number on the vibration and expressing clearly which mode occurs approximately in which frequency and which natural frequency is more destructive due to its damping ratios.

2. Material and Method

2.1 Mathematical Model

The experimental setup in this study can be shown as an example of an undamped mechanism with 6 degrees of freedom.

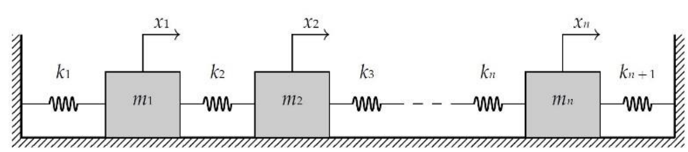

Fig. 1. A model of an undamped system with n degree of freedom

A connecting rod could be considered as if it consists of 6 different masses and each one of these masses is connected to another with k stiffness. The displacement of each mass is shown with x.

Mass, damping and stiffness matrices expresses the entire elastic structures as relating to each other using Newton's second law of motion as well as force. [16] Equation of motion of an undamped system:

$$[M]\{\ddot{x}\}+[K]\{x\}=\{0\} \tag{1}$$

The time-dependent general solution of the second-order differential equation:

$$\{x(t)\} = \{\bar{X}\}e^{i\omega t} \tag{2}$$

Considering two equations together:

$$\left[[\mathrm{K}] - \omega^2[M]\right]\{\bar{X}\}e^{i\omega t} = \{0\} \tag{3}$$

As $e^{i\omega t} \neq 0$ in every t moment:

$$[[\mathrm{K}] - \omega^2[M]]\{\bar{X}\} = \{0\} \tag{4}$$

That is the equation identifies the eigenvalue problem.

$$det[[\mathrm{K}] - \omega^2[M]] = 0 \tag{5}$$

Equation 5 is the characteristic equation of the system. ω_1, ω_2, ω_3,…, ω_n are the undamped natural frequencies of the system.

When these natural frequencies is taken into Equation 4, mode shapes which are shown as $\{\psi_r\}, (r = 1,2,\ldots,n)$ are obtained. For all of the r numbers, both of ω_r and $\{\psi_r\}$ are called vibrational modes.

r and s are random numbers. For the r and s modes, Equation 4 can be written as:

$$[[\mathrm{K}] - \omega_r{}^2[M]]\{\psi_r\} = \{0\} \tag{6}$$

And

$$[[\mathrm{K}] - \omega_s{}^2[M]]\{\psi_s\} = \{0\} \tag{7}$$

From the Equations 6 and 7:

$$(\omega_r{}^2 - \omega_s{}^2)\{\psi_s\}^T[\mathrm{M}]\{\psi_r\} = 0 \tag{8}$$

In case of the condition of r=s:

$$\{\psi_s\}^T[\mathrm{K}]\{\psi_r\} = \omega_r{}^2\{\psi_s\}^T[\mathrm{M}]\{\psi_r\} \tag{9}$$

It is possible to express Equation 9 as:

$$\omega_r{}^2 = \frac{\{\psi_s\}^T[\mathrm{K}]\{\psi_r\}}{\{\psi_s\}^T[\mathrm{M}]\{\psi_r\}} = \frac{k_r}{m_r} \tag{10}$$

If the equations are arranged with mass and stiffness matrixes separately:

$$\{\psi\}^T[\mathrm{M}]\{\psi\} = \begin{bmatrix} \ddots & & \\ & m_r & \\ & & \ddots \end{bmatrix}$$
$$\{\psi\}^T[\mathrm{K}]\{\psi\} = \begin{bmatrix} \ddots & & \\ & k_r & \\ & & \ddots \end{bmatrix} \tag{11}$$

Instead of Equation 11, it can be expressed with a more general equation:

$$\{\phi\}^T[\mathrm{K}]\{\phi\} = [I] \tag{12}$$

[I] means identity matrix and $\{\phi\}$ means mass-normalised modal matrix. ($\{\phi_r\} = \gamma_r\psi_r$) expresses the mode shape vectors. With some arrangements, Equation 13 is obtained:

$$\{\phi\}^T[\mathrm{M}]\{\phi\} = [I]$$
$$\{\phi\}^T[\mathrm{K}]\{\phi\} = \begin{bmatrix} \ddots & & \\ & \omega_r{}^2 & \\ & & \ddots \end{bmatrix} \tag{13}$$

Free vibration solution:

$$\{x(t)\} = \{\phi\}\{q(t)\} \tag{14}$$

Substituted in Equation 1:

$$[\mathrm{M}]\{\phi\}\{\ddot{q}(t)\} + [\mathrm{K}]\{\phi\}\{q(t)\} = \{0\} \tag{15}$$

With some arrangements:

$$\{\ddot{q}(t)\} + \begin{bmatrix} \ddots & & \\ & \omega_r{}^2 & \\ & & \ddots \end{bmatrix}\{q(t)\} = \{0\} \tag{16}$$

This equation shows n separate equation of motion with a single degree of freedom. [17]

2.2 Equipment and Methods in Experimental Modal Analysis

2.2.1 Equipment

In this study, a connecting rod that belongs to a four-stroke one-cylinder diesel engine is examined.

In Experimental Modal Analysis data collecting device and software, impact hammer and accelerometer could be used. In this study, DataPhysics Quattro electronic data collecting device, SignalCalc 240 Dynamic Signal Analyzer software, Dytran Model: 3225M24 accelerometer and PCB Model: 086C03 impact hammer are used. The purpose of the experiment is to obtain the Frequency Response Function (FRF). The accelerometer provides the data of displacement. Time response expresses which displacement value is occurred in which time value. The Fourier Transformation is applied to the time signal and transforms the time signal to the frequency response. That means the transformed time signal in the frequency domain is called FRF.

Fig. 2. Dytran Model: 3225M24 accelerometer [18]

Fig. 3. PCB Model:086C03 impact hammer [19]

2.2.2 Test Object Fixing Methods

In this study, the test object is hung with an elastic spring. In Experimental Modal Analysis, there are three different fixing methods. If the test object is not fastened or attached to anything and the test object is free in terms of the motion to all directions, this fixing type is called the free condition. It has to be considered that the free condition is basically a theoretical definition. Due to the impossibility of remaining a steady and suspended position on the space for any object, the test object should be hung with a very elastic spring. If the test object is fixed from a couple of spots that belong to the test object, this fixing type is called the grounded condition. If the test object is tested in the structure or system which the test object normally operates in, this fixing type is called the in situ condition. As used in many other studies, the free condition is used in this study. The importance of this fixing method is that there is no movement restriction for the test object so that the mechanism is undamped and has 6 degrees of freedom. [20]

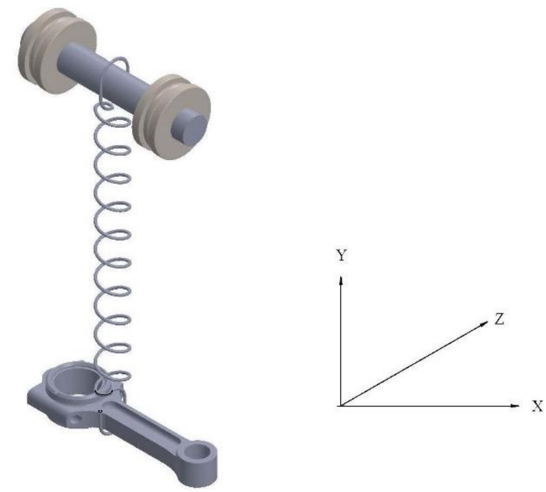

Fig. 4. The vibratory motion of the connecting rod is rotation and translation in x,y and z axis

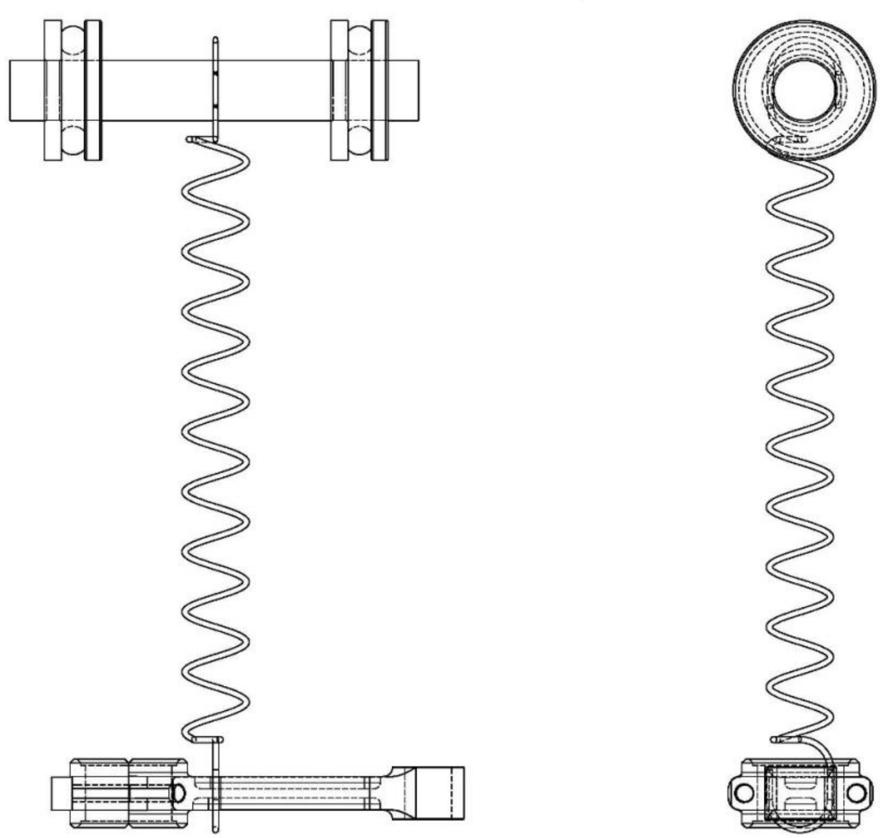

Fig. 5. Full-scale technical drawing of the experimental setup

2.2.3 Roving Accelerometer and Roving Impact Hammer Methods

Two important methods come forward to obtain the FRF graph. Firstly, some issues have to be aware of while using any of these methods: In order to select adequate equipment and devices, the frequency range of the structure or system could be simulated with specific simulation software, trial and error method could be used especially while choosing one of these roving methods or some experienced specialist could advise being able to experiment more correctly. The test object is divided to equal parts in both of these methods. For every one of these equal parts, one spot is specified. In Roving Accelerometer Method, while always the same spot is hit with an impact hammer, the spot where the accelerometer is placed changes for every single measurement. In Roving Impact Hammer Method, while always the accelerometer is placed to the same spot, the spot that is hit with the impact hammer changes for every single measurement. For both of these methods, it has to be taken into account that the weight of the accelerometer or accelerometers has to be lower than 5% of the weight of the test object. [21] In this study, the Roving Impact Hammer Method is used, because of the difficulties that are occurred while placing or replacing the accelerometers.

Besides it must be understood that the accelerometer in this study takes measurement only in the y axis which could be seen in Fig. 4.

2.2.4 Damping Ratio Estimation

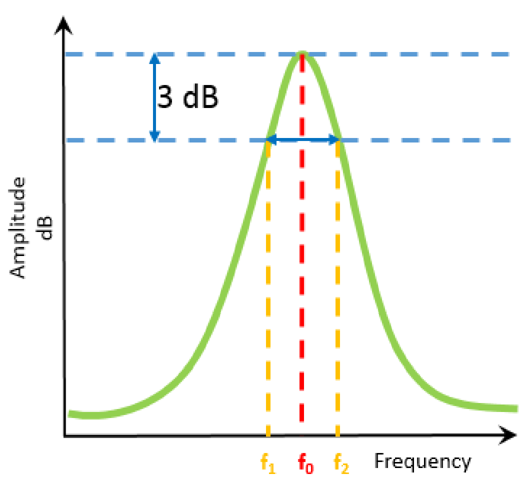

Fig. 6. Necessary parameters for the quality factor [22]

Damping demonstrates the energy dissipations that the material has in periodic stress conditions. A couple of varied parameters are derived while defining the damping for FRF. One of these parameters is the Quality Factor. The quality factor is calculated as proportioning the frequency of the peak to the frequency difference of the two points that coincide with the difference of the 3 dB amplitude points in the graph. Briefly, the proportion of the peak frequency to the frequency width around peak frequency means the quality factor. In the FRF graph, if the frequency curve peaks wider, then the damping increases and the quality factor decreases with the same ratio. If the damping is higher, the destruction of the material would be faster. The other parameter is the damping ratio that is actually calculated in this work. As it might be expected, the damping ratio increases if the damping increases. So, the damping ratio is inversely proportional to the quality factor.

$$\eta = 1/Q = 2\zeta \tag{18}$$

η = Loss factor
Q = Quality factor
ζ = Damping ratio

$$Q = \frac{f_0}{f_2 - f_1} \tag{19}$$

Rearranging the Equation 18: [22]

$$\zeta = \frac{1}{2Q} \tag{20}$$

2.3 Modal Analysis with Finite Element Method

The Finite Element Method is used with the ANSYS program. The connecting rod used in the Experimental Modal Analysis is drawn and transferred to the ANSYS program. Then theoretical Modal Analysis is carried out with the Modal module. In this work, as the free fixing method is used, it has not to be chosen any Fixed Support in the program. After getting results, the modes and the natural frequencies that belong to these modes are obtained.

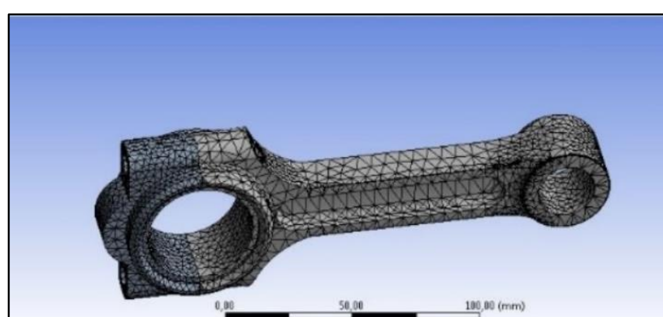

Statistics	
Nodes	44130
Elements	25673

Fig. 7. Details of meshing

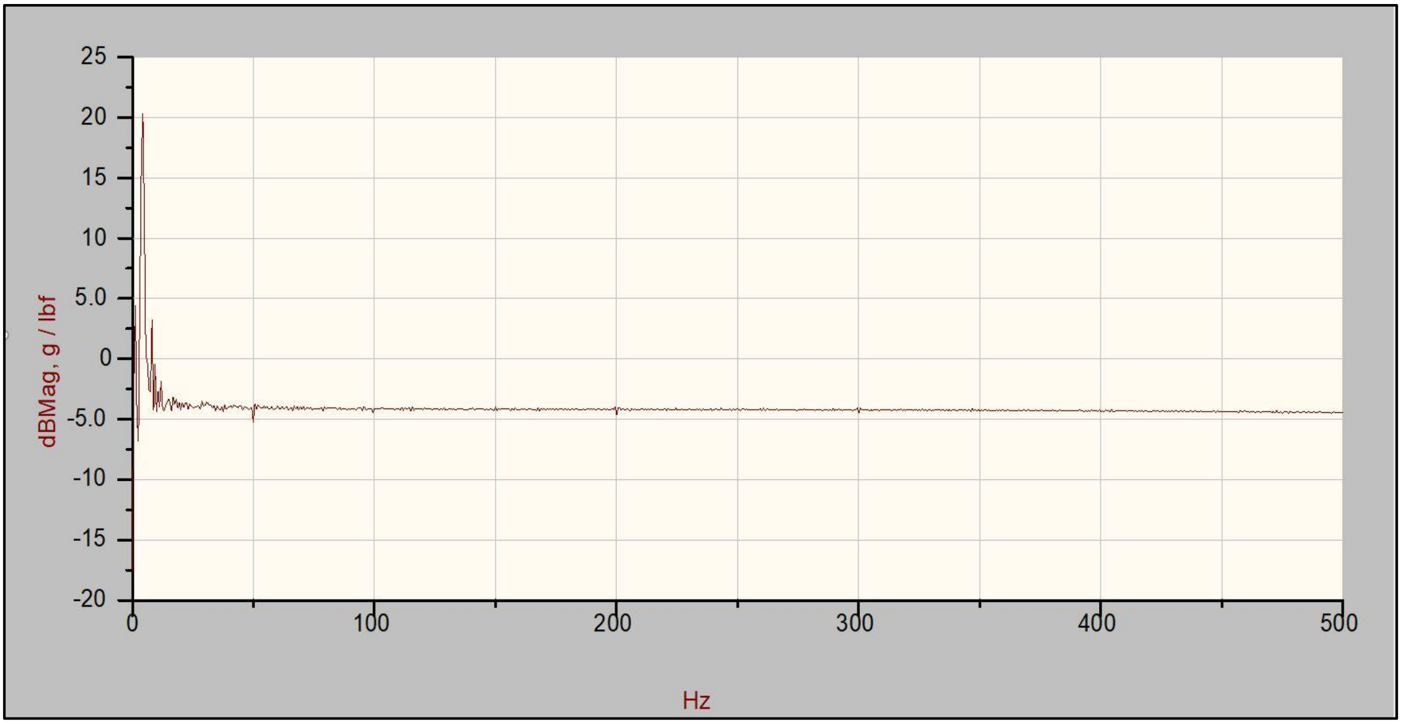

Fig. 8. FRF graph obtained with SignalCalc 240 Dynamic Signal Analyzer Software

3. Results

3.1 Experimental Modal Analysis Results

The graph showed in Fig.8 that is obtained from the SignalCalc program is shown completely first and then the zoomed-in version to the natural frequencies is shown.

The coherence function graph is a criterion for the quality of the obtained FRF graph. If the graph converges to the value of 1, it shows that in every repetition of the measurement, the same values are obtained. [23]

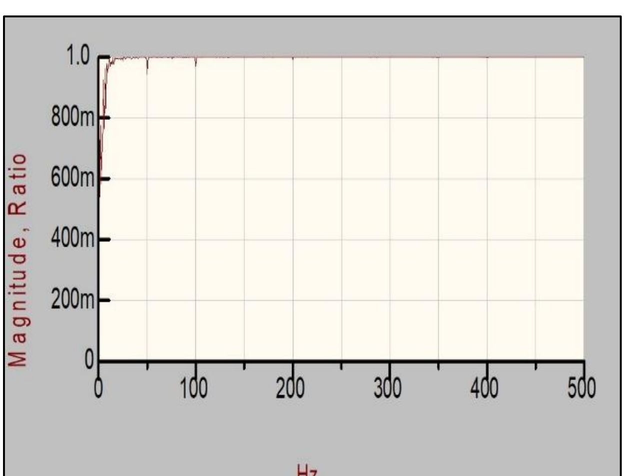

Fig. 9. Graph of the coherence function

The FRF is a complex function. Therefore the FRF consists of Real and Imaginary parts. The amplitude-frequency graph which is given above could be expressed based on the equation below:

$$Amplitude = \sqrt{Real^2 + Imaginary^2} \tag{21}$$

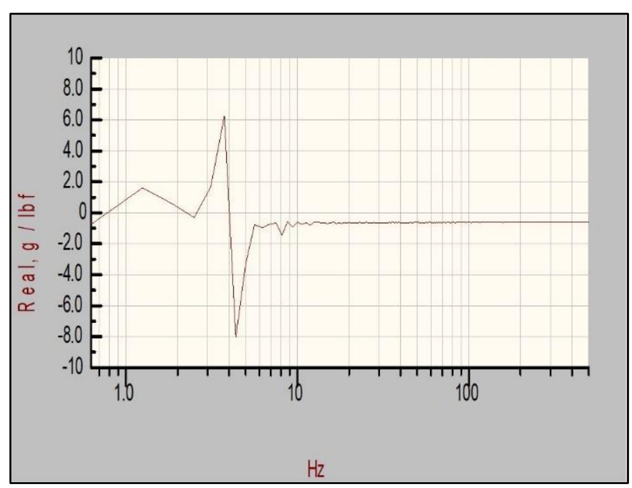

Fig. 10. Graph of the real part of FRF

Consequently, the graphs of the real and imaginary parts that constitute the amplitude function are given in Fig. 10 and Fig. 11 and these results have to be known.

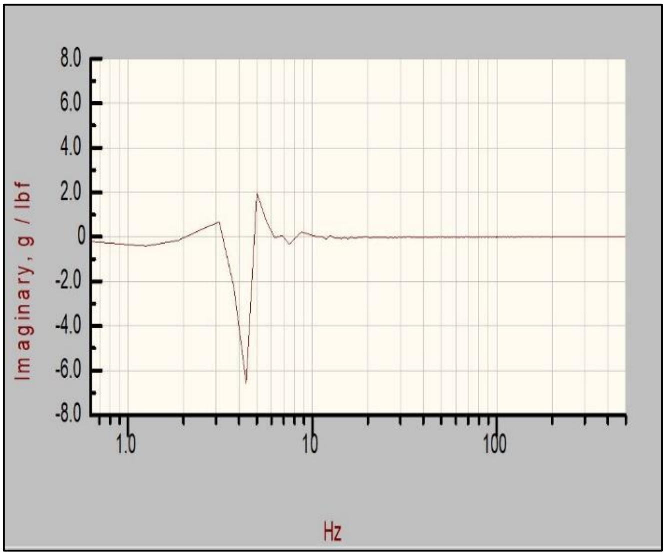

Fig. 11. Graph of the imaginary part of FRF

In Fig. 12, zoomed-in graph of the amplitude-frequency function, the x-axis shows the frequency values which have a unit of Hertz and the y-axis shows that the amplitude value that is the proportion of the acceleration response to the input force, and the amplitude has a unit of g/lbf.

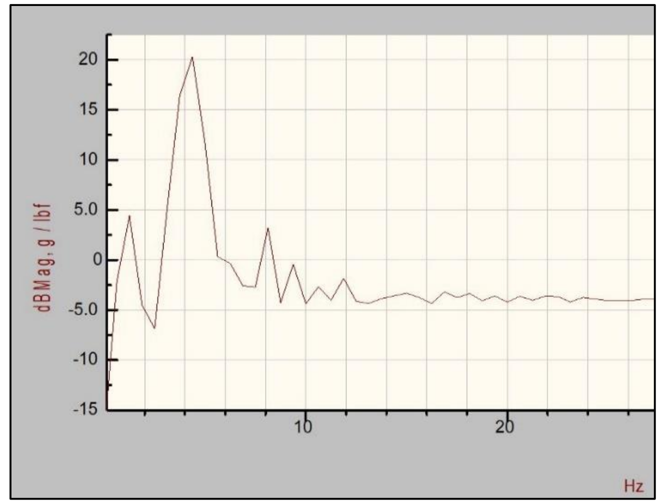

Fig. 12. Zoomed-in FRF graph that clearly shows natural frequency values

According to the graph, obtained natural frequencies are shown in Table 1:

Table 1. Natural frequencies obtained by Experimental Modal Analysis

Mode	Natural Frequency (Hz)
1	1,25
2	4,38
3	8,13

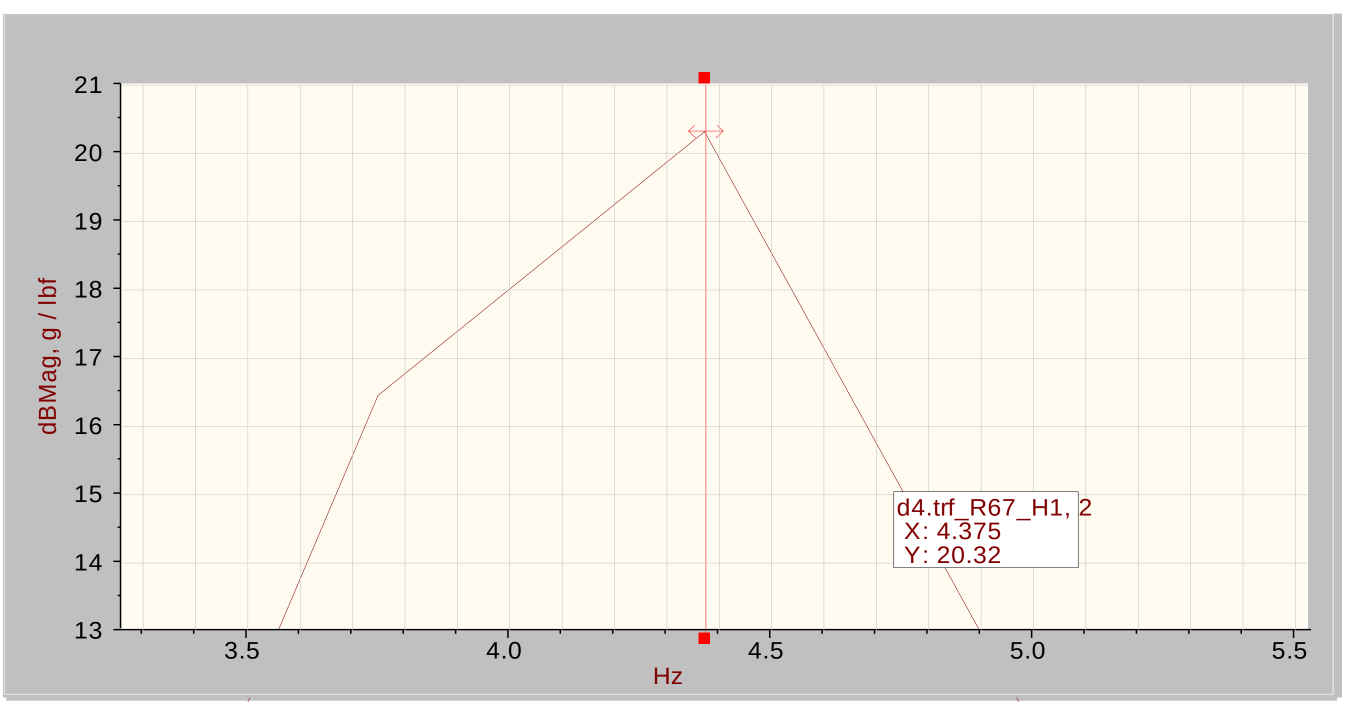

Fig. 13. Necessary parameters for the quality factor.

3.2 Damping Ratio Calculation

The damping ratio is calculated as the example given below for the second mode. In Fig 13, the FRF graph that shows the peak point of the second mode is given.

From this graph, obtained frequencies and the magnitude values are arranged in Table 2.

Table 2. Frequency and amplitude values nearby the peak of Mode 2

Frequency (Hz)	dBMag (g/lbf)
3,75	16,45
4,38	20,32
5,00	11,64

The peak point has a magnitude of 20,32 g/lbf. Then the following question has to be asked: What are the two frequency values when the magnitude has the value of 17,32 g/lbf? f1 and f2 values which are mentioned in Equation 19 would be obtained by using interpolation because the lines in the graph are linear. These calculations are done also for modes 1 and 3 and Table 3 is created:

Table 3. Damping ratio and quality factor values that belong to all modes

Mode	Damping Ratio (ζ)	Quality Factor (Q)
1	% 19,766	2,5296
2	% 8,0116	6,241
3	% 3,4839	14,3317

3.3 Finite Element Method Results

The connecting rod is drawn and transferred to the ANSYS Modal module. Required number of mesh is created. Then the connecting rod is analyzed in accordance with the free fixing method. The results are given in Table 4.

Table 4. Natural frequencies obtained by ANSYS program

Mode	Natural Frequency (Hz)
1	0,045745
2	8,3861
3	8,9434
4	1367,5
5	1582,4
6	2399,3

In Table 5, all the results obtained are presented comparatively

Table 5. Natural frequencies, damping ratios and quality factor values

Mode	Natural Frequency (Hz) with EMA	Natural Frequency (Hz) with FEM	Damping Ratio (ζ)	Quality Factor (Q)
1	1,25	0,045745	% 19,766	2,5296
2	4,38	8,3861	% 8,0116	6,241
3	8,13	8,9434	% 3,4839	14,3317

Obtained mode shapes are shown in the figures below:

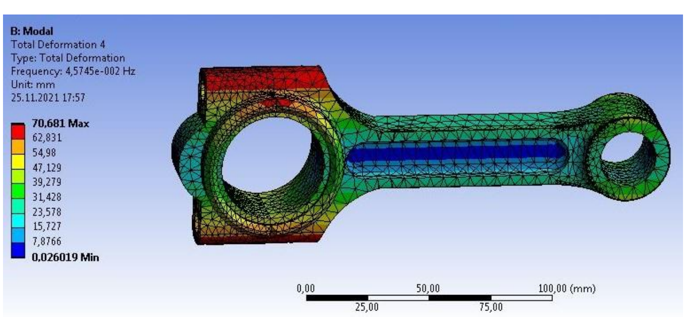

a) Mode 1

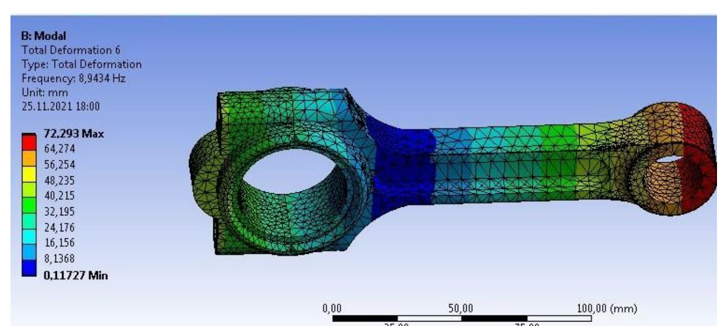

c) Mode 3

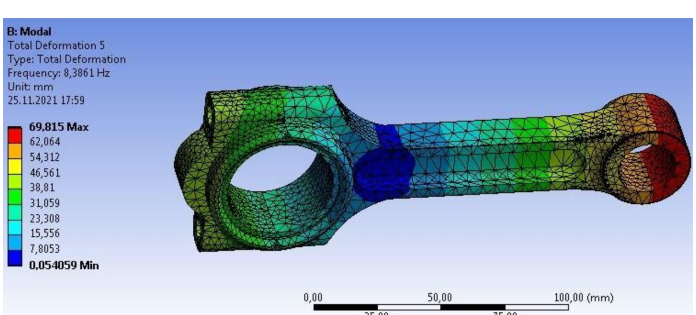

b) Mode 2

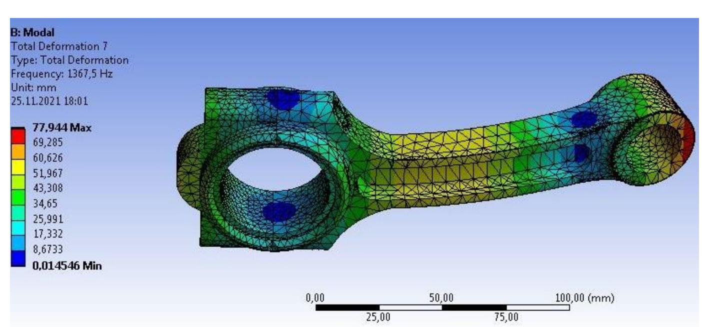

d) Mode 4

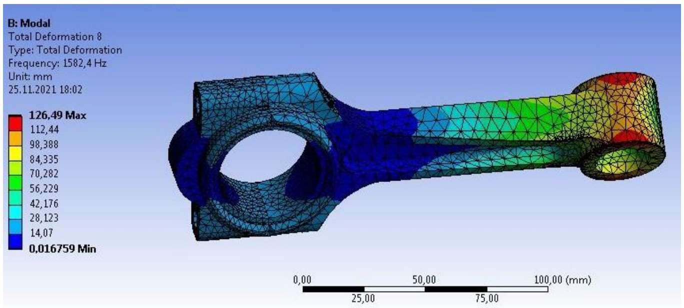

e) Mode 5

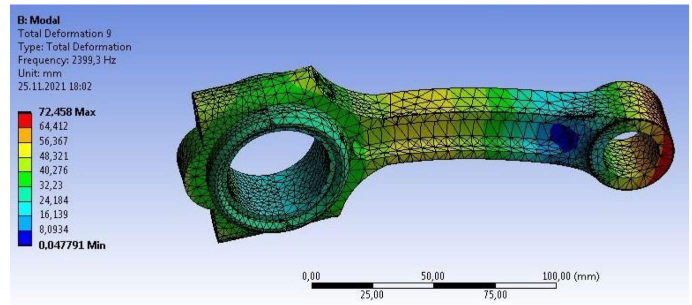

f) Mode 6

Fig 13. Mode shapes for all modes

Mode shapes are obtained from ANSYS as total deformation which gives deformation data in the x, y, and z-axis. In the first three modes, deformations mostly occurred only along the z-axis. Also, the deformations occur increasing inside to outside. Therefore, an obvious mode shape does not take place for the first 3 modes. In the last three modes, bending, torsion, and bending mode shapes were observed, respectively. It should be noted that the bending occurs in different axes in the two bending modes.

4. Conclusions

The results are nearly similar except the second modes in the results obtained with Experimental Modal Analysis and FEM. First of all, it should be known that the evaluations will be made based on the following information:

- It is taken into account that the idle speed should be between 600-1000 rpm in passenger cars. [24]
- 1 Hz = 60 rpm

Considering both assumptions are correct for all modes, the following evaluations can be made:

Unit conversations are made for the data obtained from Experimental Modal Analysis results. It is calculated 75 rpm for the 1st mode, 262,8 rpm for the 2nd mode and 487,8 rpm for the 3rd mode.

Unit conversations are made for the data obtained from FEM results. It is calculated 2,7447 rpm for the 1st mode, 503,166 rpm for the 2nd mode, 536,604 rpm for the 3rd mode, 82050 rpm for the 4th mode, 94944 rpm for the 5th mode, 143958 rpm for the 6th mode.

The rpm values of the natural frequencies of the 1st, 2nd, and 3rd modes remained below 600 rpm, which is the minimum value of the idle speed, which is known to be the lowest speed of the engine. The 4th, 5th and 6th mode values obtained with FEM have reached such high revolutions that they cannot be the operating speed of an engine. Accordingly, the natural frequencies of the connecting rod were obtained according to the engine operating conditions.

These differences in Table 5 are originated from fixing the test object in Experimental Modal Analysis and ANSYS. In Experimental Modal Analysis, it is almost impossible to analyze without fixing the object to anywhere. Because of that, an elastic spring is used for the purpose of being able to move and rotate in all possible directions. However, in ANSYS, it is possible to analyze the test object without attaching anywhere. In practice, it is assumed that EMA gives more accurate results. Because of the inconsistencies between the data of EMA and finite element results, numerous amount of calculating methods has been developed to update FEM. [25] So that the applications that are related to FEM updating with the experimental results are carried out based on this information. In further studies, FEM updating applications could be examined.

The 1st and 3rd modes gave similar results. Differences were observed between experimental results and results from ANSYS only in mode 2. These results show that both modal analysis results confirm each other. For the 2nd and 3rd modes evaluated in the ANSYS results, it is seen that the natural frequency values are very close. It is observed that the damping ratios decrease as the frequency values increase. It is seen in the Table 3 that the most critical situation for the connecting rod occurs at low frequencies. As it is mentioned in the Section 2.2.4, if the damping is higher, the destruction of the material would be faster. Care should be taken to ensure that engine operating speeds are above critical speeds. It has been concluded that the engine should not especially be operated at critical speeds.

Nomenclature

[M]	: mass matrix
[K]	: stiffness matrix
{x}	: vector of displacements
Ω	: frequency (Hz)
$\{\psi_r\}$	: mode shapes
[I]	: identity matrix
$\{\phi\}$	: mode shape vectors

Conflict of Interest Statement

The authors declare that there is no conflict of interest in the study.

CRediT Author Statement

Abdurrahman Karabulut: Conceptualization, Supervision, **Bahri Şamil Korkmaz:** Conceptualization, Writing-original draft

References

[1] Pulkrabek WW. Engineering fundamentals of the internal combustion engine. Prentice Hall. 2007; 15.

[2] Çetinkaya S. Taşıt mekaniği. Nobel Yayın Dağıtım. 2010; 23.

[3] Grohe H. Otto ve Dizel Motorları. Bilim Teknik Yayınevi. 1999; 6, 249, 250.

[4] https://www.uml.edu/docs/apr98_tcm18-189811.pdf, (30.11.2021)

[5] More HC, Mishra H. Natural Frequency Exploration of Connecting Rod By Fea Modal Analysis And Experimental Modal Analysis. International Journal of Research Publications in Engineering and Technology [IJRPET]. 3, 22-25.

[6] Nale RS, Kulloli VK. Vibrational analysis and optimization of connecting rod. International Research Journal of Engineering and Technology. 2018; (05), 07.

[7] Tong Z, Liu H, Zhu F. Modal analysis for connecting rod of reciprocating mud pump. In International Conference on Artificial Intelligence and Computational Intelligence Springer, Berlin, Heidelberg. 2009; 215-220.

[8] Manda M, Kola R, Karunakarreddy K. Modal analysis of a connecting rod using ANSYS. International Journal of Mechanical Engineering. 2017; 4, 30-35.

[9] Kumar KS. Design and analysis of IC engine piston and piston-ring on composite material using Creo and Ansys software. Journal of Engineering and Science. 2016; 1(1), 39-51.

[10] Zheng B, Zhang J, Yao Y. Finite element analysis of the piston based on ANSYS. In 2019 IEEE 3rd Information Technology, Networking, Electronic and Automation Control Conference (ITNEC). IEEE. 2019; March. 1908-1911

[11] Patil S, Patil, SF, Karuppanan S. Modal and Fatigue Analysis of a Camshaft using FEA. International Journal of Applied Engineering Research. 2013; 8(14), 1685-1694.

[12] Thriveni K, Chandraiah BJ. Modal analysis of a single cylinder 4-stroke engine crankshaft. International Journal of Scientific and Research Publications. 2013; 3(12).

[13] Naghate S, Patil S. Modal analysis of engine mounting bracket using FEA. International journal of engineering research and applications (IJERA). 2012; 2(4), 1973-1979.

[14] Nuraini AA, Mohd Ihsan AKA, Nor MJM, Jamaluddin N. Vibro-acoustic analysis of free piston engine structure using finite element and boundary element methods. Journal of Mechanical science and Technology. 2012; 26(8), 2405-2411.

[15] Chaudhary YV, Walsh S, Singh OP, Subramoniam C. Optimum knock sensor location through experimental modal analysis of engine cylinder block. 2011.

[16] Marwala, T. Finite-element-model updating using computional intelligence techniques: Applications to structural dynamics. Springer-Verlag London Limited. 2010; 69.

[17] Maia NMM, e Silva JMM. Theoretical and experimental modal analysis. Research Studies Press. 50-56.

[18] https://www.dytran.com/Model-3225M24T-Miniature-Accelerometer-with-TEDS-P1665/, (02.03.2022)

[19] https://www.pcb.com/products?model=086c03, (02.03.2022)

[20] Ewins, D. J., 1995. Modal testing: theory and practice. John Wiley & Sons. 1997; 15.

[21] Yalnızca O, Özelgin İ, Aksoy E. Esnek Volan Modal Analizi. Mühendis ve Makina. 2014; 656, 30-41.

[22] https://community.sw.siemens.com/s/article/how-to-calculate-damping-from-a-frf, (16.12.2021)

[23] https://community.sw.siemens.com/s/article/what-is-a-frequency-response-function-frf, (16.12.2021)

[24] Bennett S. Medium/heavy duty truck engines, fuel & computerized management systems, Cengage Learning. 2013; 368.

[25] Mottershead JE., Friswell MI. Model Updating in Structural Dynamics: A Survey. Journal of Sound and Vibration 1993; 167, 347–375.